A Novel Model for Link Dynamics in Planar Snake Robots Using Internal Constraint Force Sensing

Jostein Løwer[1], Irja Gravdahl[1], Damiano Varagnolo[1] and Øyvind Stavdahl[1]

***Abstract*— We consider the problem of simplifying the typically complex task of deriving dynamical mechanical models of planar snake robots. More precisely we propose a modeling strategy that assumes the possibility of measuring the constraint forces acting between adjacent links in a snake robot, something that is now technologically possible thanks to currently available compact commercial sensors. We show that this information can be used to decouple the dynamics of each link in the snake robot to build a novel dynamic model that is simpler than the typical models in the available literature, but still powerful for predicting the movements of the robots. The proposed model may help to significantly reduce the computational complexity associated with model-based control and estimation schemes compared to other established models. Besides this, we show that the proposed model exhibits multiple properties that ease performing control, identification and state estimation tasks in general. More specifically, we show that parts of the dynamics of the model can be considered to be linear with a known non-linear exogenous disturbance which can be eliminated using feed-forward control. Finally, we show that linear Kalman Filters remain the best linear unbiased estimators for part of the state even when exogenous disturbances enter non-linearly in the system.**

I. Introduction

Snake robots are mechanisms designed to mimic biological snakes, which aspire to inherit the robustness and stability properties of biological snake locomotion. Like their biological counterparts, artificial snakes move using an array of different propulsion techniques such as lateral undulation, sinus lifting and sidewinding [1]. These gaits are explained well by [2]. In principle this makes snake robots suitable for moving in and adapting to some specific unknown and challenging environments such as rubble following landslides or in collapsed buildings. As of yet, this is largely an unrealized potential. Many existing systems for Obstacle-Aided Locomotion (OAL) [3], such as in [4], [5], adapt to the environment in an implicit manner only, with little utilization of mechanical sensor information. In contrast, the present work is part of an effort to achieve efficient, robust and intelligent locomotor behavior by exploiting continually updated information about the external forces derived from constraint forces between adjacent links in the robot.

Previous works have tackled the problem of modeling the complex dynamics of a planar snake robot. [6] presents a simplified model, whereby complex parts of the robots dynamics are linearized. More recently, the kinematics of a snake robot were modeled using Geometric Algebra [7], [8], and a model was created for further research into hybrid OAL [9].

[1] Department of Engineering Cybernetics, Norwegian University of Science and Technology (NTNU), Trondheim, Norway

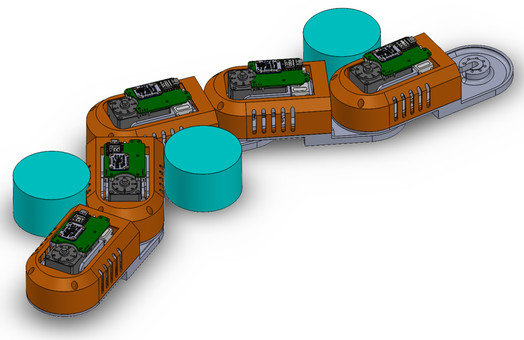

Fig. 1. A digital render of a 5-link Boa V2 snake robot.

A snake robot, being a mechanical structure consisting of joints and rigid links, can be modeled as a dynamic system. Liljebäck et.al. [10] defines a complete model of the kinematics of the robot and a set of equations describing its dynamics, building on the defined kinematics. Subsequently they provide a linearization of the dynamics and investigate the controllability properties of the model. For their complete dynamic model and its derivation the reader is referred to [10]. The Boa snake robot [11], as shown in Figure 1, is a novel experimental platform built for research into OAL. It is the latest in a family of robots which include multi-axis force sensors in each joint of the robot, making it possible to measure the constraint forces acting between the links. Boa also includes a multi-axis Inertial Measurement Unit (IMU) in each link, making it possible to extract odometric sensor data from each link. The measurement system allows for exploration into alternative ways of modeling the robot. This work presents a novel dynamical model for a planar snake robot that exploits the constraint force measurement system of the Boa, and discusses the properties and application of the model. Specifically, the contributions of this paper include:

- A novel model that incorporates constraint force measurements from the joints of the snake robot to simplify the dynamic equations, rendering parts of the dynamics linear when modeling the internal constraint forces as known exogenous disturbances.
- A feed-forward controller to eliminate the exogenous disturbance from the rotational dynamics of the robot.
- A discretization of the novel model, which under certain

conditions has the Kalman Filter as the best linear unbiased estimator for the rotational state of the model.

- A complexity analysis showing that forward computations of the novel model has a lower bound on space and computational complexity than the model in [10].

This paper is organized as follows: Section II reiterates some of the key notation on snake robot modeling, which is used in Section III to derive the novel model. Section IV defines a first-order discretization of the model, while Section V discusses the properties of the models presented in the paper.

II. Notation

The following section reiterates some of the key notation for modeling planar snake robots, defined in [10] and [11].

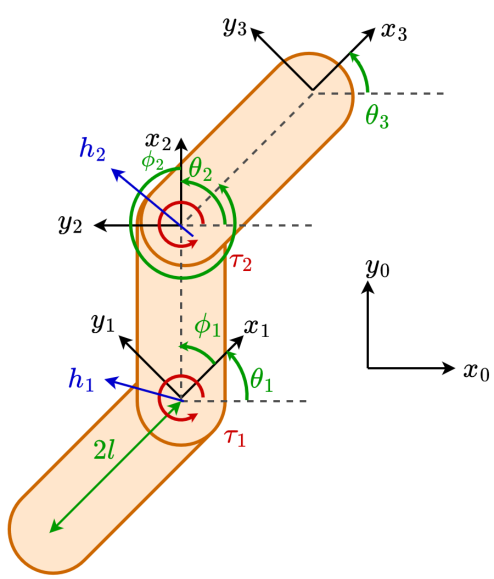

Fig. 2. The kinematics of a simple 3-link planar snake robot as seen from above. The constraint forces h_i^i (blue) are resolved in their link-local frames (black arrows). The link angles θ_i and joint angles ϕ_i (green arcs) relate the orientations of the link-local frames. The joint torque τ_i (red) is the control input of the snake robot. The link length $2l$ is shown as a green double-headed arrow.

A visualization of a planar snake robot's kinematics is shown in Figure 2. The robot consists of N links connected by $N_J = N - 1$ rotational joints whose axes of rotation are all parallel. The robot exists in a world coordinate frame (x_0, y_0). Each link of the robot has its own link local coordinate frame (x_i, y_i) where i is the link number. For the remainder of this paper, an integer superscript will denote the reference frame of the variable, and a subscript denotes the link index, e.g., $\ddot{r}_{i-1}^i$ denotes the acceleration of link $i-1$ expressed in terms of the link local frame of link i. The local frames are oriented such that the direction of the positive x_i axis coincides with the line from the axis of rotation of joint $i-1$ to that of joint i, and the y-axis points in the left transversal direction when looking in the positive x_i direction. The tail link of the robot is indexed as link 1 and the head is link N. The link angle θ_i of link i, for $i \in [1 \dots N]$, is defined as the angle between the global axis x^0 and the local axis x^i. The angle of the ith joint is denoted as ϕ_i for $i \in [1 \dots N_J]$. In the local frames, forces and torques can be schematized as in Figure 2. The relation between the link angles and the joint angles is given by

$$\phi_i = \theta_{i+1} - \theta_i \tag{1}$$

We can then define the joint angle vector $\boldsymbol{\phi}$ and the link angle vector $\boldsymbol{\theta}$ as

$$\begin{aligned} \boldsymbol{\phi} &= \begin{bmatrix}\phi_1 & \phi_2 & \dots & \phi_{N_J}\end{bmatrix}^T \\ \boldsymbol{\theta} &= \begin{bmatrix}\theta_1 & \theta_2 & \dots & \theta_N\end{bmatrix}^T \end{aligned} \tag{2}$$

and relate them by the difference matrix

$$\boldsymbol{D} = \begin{bmatrix} 1 & -1 & 0 & 0 & 0 \\ 0 & 1 & -1 & 0 & 0 \\ & & & & \\ 0 & 0 & \ddots & \ddots & \vdots \\ 0 & 0 & \dots & 1 & -1 \end{bmatrix} \in \mathbb{R}^{N_J \times N} \tag{3}$$

such that

$$\boldsymbol{\phi} = \boldsymbol{D}\boldsymbol{\theta} \tag{4}$$

In addition we also define the position of the snake robot's center of mass in global coordinates as $\boldsymbol{p}$.

III. A novel dynamical model

In [10] the torque balance for a single link i is given as

$$\begin{aligned} J\ddot{\theta}_i = \tau_{i-1} - \tau_i & \\ - l\sin\theta_i(h_{i,x}^0 + h_{i-1,x}^0) & \\ + l\cos\theta_i(h_{i,y}^0 + h_{i-1,y}^0) & \end{aligned} \tag{5}$$

where τ_i is the torque exerted by link i on link $i+1$ through joint i, $2l$ is the length of each link, and the constraint forces h are given in the world coordinate frame. The scalar J is the rotational inertia of a single link about its center of mass on the axis normal to the plane. This model assumes that torsional friction between the snake robot links and their environment is negligible, and that the external forces $\boldsymbol{f}_{e,i}$ acting on link i from the environment of the snake robot acts through the link's center of mass. In the case that torsional friction is non-negligible and the contact forces act on an arbitrary point on the link's surface, both of these effects can be embedded in the model by introducing the external link torque for link i, denoted $\boldsymbol{\tau}_{e,i}$, such that (5) would become

$$\begin{aligned} J\ddot{\theta}_i = \tau_{i-1} - \tau_i & \\ - l\sin\theta_i(h_{i,x}^0 + h_{i-1,x}^0) & \\ + l\cos\theta_i(h_{i,y}^0 + h_{i-1,y}^0) & \\ + \tau_{e,i}. & \end{aligned} \tag{6}$$

While we acknowledge the existence and effect of torsional friction and offset contact forces on the model, we choose to make the same assumptions for this model as the ones made in [10]. The effects of torsional friction can largely be mitigated through the physical design of the robot by ensuring that only a small part of the chassis of each link is in contact with the plane and by using a surface material with a low friction coefficient. The torques arising from offset external forces $\boldsymbol{f}_{e,i}$ are known to be limited in magnitude to $l||\boldsymbol{f}_{e,i}||$ which diminishes as the length $2l$ of the links decreases. As a planar snake robot is an actuated mechanism, the control inputs τ_i are typically known. With this information it is likely possible to estimate $\tau_{e,i}$ and account for its effect on the link dynamics using an *Unknown Input Observer (UIO)*, however this remains outside the scope of this paper and is a subject for future research.

In the Boa snake robot, the joint torques τ_i, as well as the link local constraint force $h^i_{i,y}$, can be measured directly by the sensor system. With slight modifications to (5) we get a torque balance that uses the link local constraint forces

$$J\ddot{\theta} = \tau_{i-1} - \tau_i + l\big(h^i_{i,y} + h^i_{i-1,y}\big). \tag{7}$$

The scalar $h^b_{a,y}$ denotes the constraint force in the y-direction from link $a+1$ on link a through joint a resolved in the local frame of link b. While the scalar $h^i_{i,y}$ can be measured directly, the constraint force $h^i_{i-1,y}$ is not explicitly known, but can be produced by rotating the force vector $\boldsymbol{h}^{i-1}_{i-1}$ from frame $i-1$ to i by applying the rotation matrix $\boldsymbol{R}^T(\phi_{i-1})$ before decomposing the force into its x and y components. This yields

$$J\ddot{\theta}_i = \tau_i - \tau_{i-1} + l\begin{bmatrix}0 & 1\end{bmatrix}\big(\boldsymbol{h}^i_i + \boldsymbol{R}^T(\phi_{i-1})h^{i-1}_{i-1}\big), \tag{8}$$

which can be rewritten in matrix notation as

$$J\ddot{\boldsymbol{\theta}} = \boldsymbol{D}^T\boldsymbol{\tau} + l\boldsymbol{\eta}_y\boldsymbol{R}_h(\boldsymbol{\phi})\boldsymbol{h}, \tag{9}$$

where $\boldsymbol{\eta}_y$ is a coordinate selection matrix, $\boldsymbol{R}_h$ is a coordinate conversion matrix, $\boldsymbol{h}$ is the link local constraint force vector and $\boldsymbol{\tau}$ is the torque vector. Furthermore these are defined as:

$$\boldsymbol{\eta}_y = \begin{bmatrix} 0 & 1 & 0 & 0 & 0 & 0 & 0 & 0 \\ 0 & 0 & 0 & 1 & 0 & 0 & 0 & 0 \\ 0 & 0 & 0 & 0 & \ddots & \ddots & \vdots & \vdots \\ 0 & 0 & 0 & 0 & \dots & \dots & 0 & 1 \end{bmatrix} \in \mathbb{R}^{N\times 2N} \tag{10}$$

$$\boldsymbol{R}_h(\boldsymbol{\phi}) = \begin{bmatrix} \boldsymbol{I} & 0 & 0 & 0 & 0 \\ \boldsymbol{R}^T(\phi_1) & \boldsymbol{I} & 0 & 0 & 0 \\ 0 & \boldsymbol{R}^T(\phi_2) & \boldsymbol{I} & 0 & 0 \\ 0 & 0 & \ddots & \ddots & 0 \\ 0 & 0 & 0 & \boldsymbol{R}^T(\phi_{N(J-1)}) & \boldsymbol{I} \\ 0 & 0 & 0 & 0 & \boldsymbol{R}^T(\phi_{NJ}) \end{bmatrix} \in \mathbb{R}^{2N\times 2N_J} \tag{11}$$

$$\boldsymbol{h} = \begin{bmatrix} h^{1\,T}_1 & h^{2\,T}_2 & \dots & h^{N_J\,T}_{N_J} \end{bmatrix}^T \in \mathbb{R}^{2N_J} \tag{12}$$

$$\boldsymbol{\tau} = \begin{bmatrix} \tau_1 & \tau_2 & \dots & \tau_{N_J} \end{bmatrix}^T \in \mathbb{R}^{N_J} \tag{13}$$

By defining the rotational state vector

$$\boldsymbol{q}_\theta = \begin{bmatrix} \boldsymbol{\theta} \\ \dot{\boldsymbol{\theta}} \end{bmatrix} \tag{14}$$

the model can be rewritten in state space form as

$$\dot{\boldsymbol{q}}_\theta = \boldsymbol{A}\boldsymbol{q}_{\boldsymbol{\theta}} + \boldsymbol{B}\boldsymbol{\tau} + \boldsymbol{C}\boldsymbol{w}_\theta(\boldsymbol{\phi}, \boldsymbol{h}), \tag{15}$$

where

$$\begin{aligned} \boldsymbol{A} &= \begin{bmatrix} \boldsymbol{0} & \boldsymbol{I} \\ \boldsymbol{0} & \boldsymbol{0} \end{bmatrix} \\ \boldsymbol{B} &= \frac{1}{J}\begin{bmatrix} \boldsymbol{0} \\ \boldsymbol{D}^T \end{bmatrix} \\ \boldsymbol{C} &= \begin{bmatrix} \boldsymbol{0} \\ \boldsymbol{I} \end{bmatrix} \\ \boldsymbol{w}_\theta(\boldsymbol{\phi}, \boldsymbol{h}) &= \frac{l}{J}\boldsymbol{\eta}_y\boldsymbol{R}_h(\boldsymbol{\phi})\boldsymbol{h}. \end{aligned} \tag{16}$$

The state space model has $\boldsymbol{q}_\theta$ as the state, $\boldsymbol{\tau}$ as the control input. The non-linear term $\boldsymbol{w}_\theta(\boldsymbol{\phi}, \boldsymbol{h})$ is further denoted $\boldsymbol{w}_\theta$ for brevity.

From [10] we have that the translational dynamics of a planar snake robot can be modeled as

$$Nm\ddot{\boldsymbol{p}} = \sum \boldsymbol{f}_{e,i} \tag{17}$$

The Boa snake robot comprises a sensor system intended to estimate the link local external forces $\boldsymbol{f}^i_{e,i}$ [11]. These can be transformed into global coordinates by the transformation $\boldsymbol{R}(\theta_i)$ as

$$\boldsymbol{f}_{e,i} = \boldsymbol{R}(\theta_i)\boldsymbol{f}^i_{e,i} \tag{18}$$

The translational dynamics of the robot can then be written in matrix notation as

$$\ddot{\boldsymbol{p}} = \frac{1}{Nm}\boldsymbol{R}_e(\theta)\boldsymbol{f}_e \tag{19}$$

where

$$\begin{aligned} \boldsymbol{R}_e(\theta) &= \begin{bmatrix} \boldsymbol{R}(\theta_1) & \dots & \boldsymbol{R}(\theta_N) \end{bmatrix} \\ \boldsymbol{f}_e &= \begin{bmatrix} \boldsymbol{f}^i_{e,i} \\ \vdots \\ \boldsymbol{f}^N_{e,N} \end{bmatrix}. \end{aligned} \tag{20}$$

By defining the translational state $\boldsymbol{q}_p$ of the snake robot as

$$\boldsymbol{q}_p = \begin{bmatrix} \boldsymbol{p} \\ \dot{\boldsymbol{p}} \end{bmatrix} \tag{21}$$

we can define rewrite (19) in state space form as

$$\dot{\boldsymbol{q}}_p = \boldsymbol{A}\boldsymbol{q}_p + \frac{1}{Nm}\boldsymbol{C}\boldsymbol{R}_e(\theta)\boldsymbol{f}_e \tag{22}$$

where the matrices $\boldsymbol{A}$ and $\boldsymbol{C}$ are the same as the ones defined in (16). By combining the translational dynamics in (22) and the rotational dynamics in (15), we get the full dynamics of a planar snake robot with the state vector

$$\boldsymbol{q} = \begin{bmatrix} \boldsymbol{q}_\theta \\ \boldsymbol{q}_p \end{bmatrix} \tag{23}$$

as

$$\begin{aligned} \dot{\boldsymbol{q}}_\theta &= \boldsymbol{A}\boldsymbol{q}_{\boldsymbol{\theta}} + \boldsymbol{B}\boldsymbol{\tau} + \boldsymbol{C}\boldsymbol{w}_\theta(\boldsymbol{\phi}, \boldsymbol{h}) \\ \dot{\boldsymbol{q}}_p &= \boldsymbol{A}\boldsymbol{q}_p + \frac{1}{Nm}\boldsymbol{C}\boldsymbol{R}_e(\theta)\boldsymbol{f}_e \end{aligned} \tag{24}$$

IV. Discretization of the Model

Assume that it is possible to sample the joint angles $\boldsymbol{\phi}$, the joint torques $\boldsymbol{\tau}$ and link local constraint forces $\boldsymbol{h}$ at a regular time interval δ_t. We denote each sampling timestep $k \in \mathbb{Z}$ and every sampled value at time $k\delta_t$ with the postscript $[k]$, e.g such that $\boldsymbol{h}[k] = \boldsymbol{h}(k\delta_t)$, and can then define

$$\boldsymbol{w}[k] = \boldsymbol{w}(\boldsymbol{\phi}[k], \boldsymbol{h}[k]) \tag{25}$$

An approximate discretized version of the model can be produced by assuming a sufficiently small time step δ_t that a first order discretization accurately represents the systems dynamics. In the following derivation, it is assumed that

$$\dot{\boldsymbol{q}} \approx \frac{\boldsymbol{q}[k+1] - \boldsymbol{q}[k]}{\delta_t} \tag{26}$$

such that Euler's method can be applied. We define the discretized stochastic state space model as

$$\begin{aligned} \boldsymbol{q}_\theta[k+1] &= \boldsymbol{A}_d\boldsymbol{q}_\theta[k] + \boldsymbol{B}_d\boldsymbol{\tau}[k] + \boldsymbol{C}_d\boldsymbol{w}[k] \\ \boldsymbol{q}_p[k+1] &= \boldsymbol{A}_d\boldsymbol{q}_p[k] + \boldsymbol{C}_d\frac{1}{Nm}\boldsymbol{R}_e(\boldsymbol{\theta}[k]) + \boldsymbol{f}_e[k] \end{aligned} \tag{27}$$

with

$$\begin{aligned} \boldsymbol{A}_d &= \boldsymbol{I} + \delta_t\boldsymbol{A} \\ \boldsymbol{B}_d &= \delta_t\boldsymbol{B} \\ \boldsymbol{C}_d &= \delta_t\boldsymbol{C} \end{aligned} \tag{28}$$

where $\boldsymbol{q}_\theta[k]$ and $\boldsymbol{q}_p[k]$ are the discrete approximations of $\boldsymbol{q}_\theta$ and $\boldsymbol{q}_p$, respectively, at timestep $\boldsymbol{k}$.

V. Properties of the Novel Model

In this section we investigate the properties of the models defined in (24) and (27) with their associated definitions.

A. Cascaded structure of the model

The structure of the state space model in (24) is shown in Fig. 3. The system can be modeled as two cascaded systems, with $\boldsymbol{\tau}$ as the input to the rotational dynamics, and its output $\boldsymbol{\theta}$ as the input to the translational dynamics. The rotational dynamics has an implicit non-linear dependency upon its own state $\boldsymbol{q}_\theta$ through the joint angles $\boldsymbol{\phi}$. However, in the likely case that $\boldsymbol{\phi}$ can be measured explicitly, the term $\boldsymbol{w}_\theta$ can be seen as a known exogenous disturbance term. In this case the rotational dynamics can be considered linear with respect to to its own state $\boldsymbol{q}_\theta$. The incorporation of the constraint forces $\boldsymbol{h}$ into the model removes the model's dependency on the angular speeds $\dot{\boldsymbol{\phi}}$ and $\dot{\boldsymbol{\theta}}$, resulting in dynamic equations which are not explicitly affected by centripetal forces or the Coriolis effect. We also note that, unlike the model given in [10], the rotational dynamics are independent of the external link forces $\boldsymbol{f}_e$ under the same assumptions.

B. Implicit enforcement of constraints

Like the established model in [10], the novel model is built upon the generalized coordinates defined in (23). Although the dynamics of the links are apparently separated, they are in fact connected by the identity $\boldsymbol{h}_i^i = -\boldsymbol{R}^T(\phi_{i-1})\boldsymbol{h}_{i-1}^{i-1}$, i.e. the choice of generalized coordinates implicitly enforces the kinematic constraints imposed on the model.

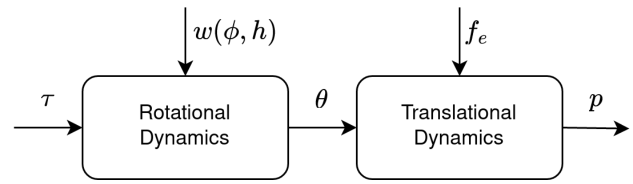

Fig. 3. A schematic of the dynamics defined in (24).

C. Elimination of exogenous disturbances from the rotational dynamics

The study of systems with exogenous disturbances such as the rotational dynamics in (24) is well developed, and is summarized in [12]. As the disturbances are known, it is possible to define a feed forward controller

$$\boldsymbol{\tau} = \boldsymbol{K}_w\boldsymbol{w}_\theta + \boldsymbol{\tau}^* \tag{29}$$

to remove the effect of the disturbances on the system, where $\boldsymbol{\tau}^*$ is the desired net torque on the joints of the robot. We choose the feed forward matrix $\boldsymbol{K}_w$ to solve

$$\boldsymbol{B}\boldsymbol{K_w}\boldsymbol{w}_\theta + \boldsymbol{C}\boldsymbol{w}_\theta = 0. \tag{30}$$

By substituting the matrices in (16) the problem reduces to

$$\boldsymbol{D^T}\boldsymbol{K_w} + \boldsymbol{I} = 0 \tag{31}$$

As the product $\boldsymbol{D}^T\boldsymbol{D}$ is non-singular, it holds that the Moore-Penrose inverse of $\boldsymbol{D}^T$ which is denoted $(\boldsymbol{D}^T)^\dagger$ solves (31) wrt. $\boldsymbol{K}_w$. The resulting controller is

$$\boldsymbol{\tau} = \boldsymbol{\tau}^* - (\boldsymbol{D}^T)^\dagger\boldsymbol{w}_\theta. \tag{32}$$

We can now plug this feedforward controller into the model in (24) resulting in an undisturbed linear system

$$\dot{\boldsymbol{q}}_\theta = \boldsymbol{A}\boldsymbol{q}_\theta + \boldsymbol{B}\boldsymbol{\tau}^*. \tag{33}$$

D. Noise properties of the feedforward controller

In this subsection we investigate the properties of the discrete model in (27) with the combined feedforward controller defined in Section V-C when the exogenous disturbance $\boldsymbol{h}[k]$ is subject to noise. Assume that the joint torque and link local constraint force measurements are affected by zero-mean Gaussian noises with known covariance $\boldsymbol{\sigma}_h^2$ such that the measured link local constraint forces $\tilde{\boldsymbol{h}}[k]$ at timestep k can be defined as

$$\tilde{\boldsymbol{h}}[k] \sim \mathcal{N}(\boldsymbol{h}[k], \boldsymbol{\sigma}_h^2). \tag{34}$$

This in turn allows us to define the noisy exogenous disturbance $\tilde{\boldsymbol{w}}_\theta[k]$ as

$$\tilde{\boldsymbol{w}}_\theta[k] = \boldsymbol{w}_\theta(\boldsymbol{\phi}[k], \tilde{\boldsymbol{h}}[k]). \tag{35}$$

As the Gaussian quality of the noise does not change under linear transformations, the distribution of $\tilde{\boldsymbol{w}}_\theta[k]$ is known to be Gaussian with a covariance and expectation that can be calculated from (15) as

$$\tilde{\boldsymbol{w}}_\theta[k] \sim \mathcal{N}(\boldsymbol{w}_\theta[k], \boldsymbol{\sigma}_w^2) \tag{36}$$

$$\boldsymbol{\sigma}_w^2 = l^2 \boldsymbol{\eta}_y \boldsymbol{R}_h(\boldsymbol{\phi}) \boldsymbol{\sigma}_h^2 (\boldsymbol{\eta}_y \boldsymbol{R}_h(\boldsymbol{\phi}))^T. \tag{37}$$

These calculations assume that the joint angles $\boldsymbol{\phi}$ has negligible noise, which may be a reasonable assumption in most systems, as high resolution rotary encoders are known to purvey little-to-no measurement noise.

By inserting the controller from (29) using the noisy disturbance $\tilde{\boldsymbol{w}}_\theta[k]$ into the rotational dynamics from (27), we get the system

$$\begin{aligned} \boldsymbol{q}_\theta[k+1] = \boldsymbol{A}_d \boldsymbol{q}_\theta[k] \\ + \boldsymbol{B}_d(\boldsymbol{\tau}^* - (\boldsymbol{D}^T)^\dagger) \tilde{\boldsymbol{w}}_\theta[k] \\ + \boldsymbol{C}_d \boldsymbol{w}_\theta[k], \end{aligned} \tag{38}$$

which reduces to a linear system with Gaussian zero mean noise

$$\boldsymbol{q}_\theta[k+1] = \boldsymbol{A}\boldsymbol{q}_\theta[k] + \boldsymbol{B}_d \boldsymbol{\tau}^*[k] + \boldsymbol{\xi}[k] \tag{39}$$

with

$$\boldsymbol{\xi}[k] \sim \mathcal{N}(0, \boldsymbol{\sigma}_w^2). \tag{40}$$

Equation (39) represents a linear process model with zero-mean Gaussian noise as defined in [13], which is used to form the basis for a *Kalman Filter*.

E. Optimality of the Kalman Filter as the rotational state estimator

We now introduce an observation model $\boldsymbol{z}_\theta[k]$ that makes it possible to measure the rotational state $\boldsymbol{q}_\theta[k]$ as a linear combination of the states through the measurement function

$$\boldsymbol{z}_\theta[k] = \boldsymbol{H}\boldsymbol{q}_\theta[k] + \boldsymbol{v}[k], \tag{41}$$

where

$$\boldsymbol{v}[k] \sim \mathcal{N}(0, \boldsymbol{\sigma}_v^2). \tag{42}$$

One such implementation of $\boldsymbol{H}$ and $\boldsymbol{v}[k]$ is found in the Boa snake robot, where it is possible to measure the joint angles $\boldsymbol{\phi}$ through rotary encoders in the joints of the robot, and $\boldsymbol{q}_\theta$ using a gyroscope and magnetometer embedded in each link. The resulting measurement model then becomes

$$\boldsymbol{H} = \begin{bmatrix} \boldsymbol{D} & \boldsymbol{0} \\ \boldsymbol{I} & \boldsymbol{0} \\ \boldsymbol{0} & \boldsymbol{I} \end{bmatrix} \tag{43}$$

For the discrete model in (39) with a measurement model structure as in (41) resulting in an observable system, the Kalman Filter is the *Best Linear Unbiased Estimator (BLUE)* for the state $\boldsymbol{q}_\theta[k]$ [13]. The implication of this is that, even if the model (27) is not linear wrt. $\boldsymbol{h}[k]$ and $\boldsymbol{\phi}[k]$, the Kalman Filter is still the BLUE estimator for the state $\boldsymbol{q}_\theta[k]$ if the constraint force measurements $\tilde{\boldsymbol{h}}[k]$ are unbiased and Gaussian. The unbiasedness and optimality of the estimator is dependent on that the measurements of the joint angle $\boldsymbol{\phi}$ are known and near noiseless.

F. Computational complexity

The following subsection uses big-$\mathcal{O}$ notation as defined in [14]. A property of the novel model is its ability to reduce computational complexity in calculations. Consider the state space model defined in (24). The band sparse structure of the matrices $\boldsymbol{A}$, $\boldsymbol{B}$, $\boldsymbol{C}$ and $\boldsymbol{\eta}_y \boldsymbol{R}_h(\boldsymbol{\phi})$ arises from the fact that the constraint force measurements decouples the dynamics of the links, making the dynamics of a single link independent of the dynamics of the adjacent links in the robot. Band sparse matrices have a number of non-zero elements limited by $\mathcal{O}(N)$ as opposed to the matrices used in the model in [10] where most matrices are dense and the number of non-zero elements is limited by $\mathcal{O}(N^2)$. We also note that the matrix $\boldsymbol{R}_e$ has a number of non-zero elements limited by $\mathcal{O}(N)$ even if it is not band-sparse.

For the model in (24), the computation of $\dot{\boldsymbol{q}}$ is upper bounded in computational complexity by the matrix multiplication operation which is normally bounded by $\mathcal{O}(N^3)$. As all matrices included in this computation are bandsparse, the computational complexity of $\dot{\boldsymbol{q}}$ can be reduced to $\mathcal{O}(N^2)$ [15]. Similarly, the space complexity of the model is upper bounded by $\mathcal{O}(N)$. The savings in computation and space complexity using the novel model can be useful when running control or state estimation algorithms on systems limited in storage and computational power such as in embedded microcontrollers.

VI. Conclusions

We derived and proposed a novel model for planar snake robots that has linear rotational dynamics with known exogenous disturbances, and shown how these disturbances may be eliminated using rudimentary feed forward control actions. We have also discussed how a stochastic discretization of the model can be used to prove that, under certain conditions, linear Kalman Filtering is the minimum variance linear unbiased estimation technique for the rotational state of the robot. Finally, we have shown how the novel model leads to lower computational and space complexity requirements than using other established models.

References

[1] J. Gray, "The mechanism of locomotion in snakes," *Journal of experimental biology*, vol. 23, no. 2, pp. 101–120, 1946.

[2] R. Ariizumi and F. Matsuno, "Dynamic analysis of three snake robot gaits," *IEEE Transactions on Robotics*, vol. 33, no. 5, pp. 1075–1087, 2017.

[3] A. A. Transeth, "Modelling and control of snake robots," Ph.D. dissertation, NTNU, 2008.

[4] T. Kano, N. Matsui, and A. Ishiguro, *3D Movement of Snake Robot Driven by Tegotae-Based Control*. Springer, 07 2019, pp. 346–350.

[5] P. Liljeback, K. Pettersen, and O. Stavdahl, "Modelling and control of obstacle-aided snake robot locomotion based on jam resolution," in *Proceedings / IEEE International Conference on Robotics and Automation*, 06 2009, pp. 3807 – 3814.

[6] P. Liljebäck, K. Y. Pettersen, Ø. Stavdahl, and J. T. Gravdahl, "A simplified model of planar snake robot locomotion," in *2010 IEEE/RSJ International Conference on Intelligent Robots and Systems*, 2010, pp. 2868–2875.

[7] J. Hrdina, A. Návrat, and P. Vašík, "Control of 3-link robotic snake based on conformal geometric algebra," *Advances in Applied Clifford Algebras*, vol. 26, pp. 1069–1080, 2016.

[8] J. Hrdina, A. Návrat, P. Vašík, and R. Matoušek, "Geometric control of the trident snake robot based on cga," *Advances in Applied Clifford Algebras*, vol. 27, pp. 633–645, 2017.

[9] I. Gravdahl, Ø. Stavdahl, A. Koushan, J. Løwer, and K. Y. Pettersen, "Modeling for hybrid obstacle-aided locomotion (hoal) of snake robots," *IFAC-PapersOnLine*, vol. 55, no. 20, pp. 247–252, 2022.

[10] P. Liljebäck, K. Y. Pettersen, Ø. Stavdahl, and J. T. Gravdahl, *Snake robots: modelling, mechatronics, and control*. Springer Science & Business Media, 2012.

[11] J. Lower, I. Gravdahl, D. Varagnolo, and O. Stavdahl, "Proprioceptive contact force and contact point estimation in a stationary snake robot," in *Proceedings / SYROCO 2022*. IFAC, 2022.

[12] M. V. Khlebnikov, "Control of linear systems subjected to exogenous disturbances: Combined feedback," *IFAC-PapersOnLine*, vol. 49, no. 13, pp. 111–116, 2016, 12th IFAC Workshop on Adaptation and Learning in Control and Signal Processing ALCOSP 2016. [Online]. Available: https://www.sciencedirect.com/science/article/pii/S2405896316312241

[13] R. E. Kalman, "A new approach to linear filtering and prediction problems," *Transactions of the ASME–Journal of Basic Engineering*, vol. 82, no. Series D, pp. 35–45, 1960.

[14] I. Chivers and J. Sleightholme, "An introduction to algorithms and the big o notation," in *Introduction to programming with Fortran*. Springer, 2015, pp. 359–364.

[15] T. A. Davis, *Direct methods for sparse linear systems*. Society for Industrial and Applied Mathematics, 2006.